PUSH-OUT TESTS ON BOREHOLE PLUGS

John C. Stormont
Jaak J.K. Daemen
Department of Mining and Geological Engineering
University of Arizona
Tucson, Arizona 85721

ABSTRACT

Over 100 push-out tests on cement plugs cast in boreholes in rock samples were performed in order to gain information about the mechanical strength of the borehole plug-rock system. The results, although quite variable, indicate a high peak strength and significant residual strength (30-50% of peak strength). The shear stress distribution for a completely elastic response was derived to be exponential. A frictional model of the interface, $\tau = c + \sigma\tan\phi$, allows study of the components of the strength. This strength, when integrated over the surface of the plug, provides a theoretical strength of the entire interface reasonably close to the experimental results. In-situ plug behavior will differ from laboratory plugs; however, cement plugs at repository depths should have strengths well in excess of anticipated loads.

INTRODUCTION

Current plans by the Department of Energy call for the disposal of radioactive waste deep (approximately 1000 meters) in underground repositories.[1] To ensure that migration of radionuclides to the accessible environment is prevented, all penetrations (boreholes, shafts, and tunnels) must be sealed adequately. The seal or plug may be subjected to a number of possible loading mechanisms, the most likely one being water pressure.[2]

There is a serious lack of evidence as to the strength or integrity of these seals under loading. This study, as part of ongoing research at the University of Arizona sponsored by the Nuclear Regulatory Commission, will determine whether the strength of the seal is adequate for the maximum anticipated loads of repository depths and conditions. In addition, important variables and mechanisms of the strength will be identified.

LABORATORY TESTING

The objective of the push-out experiment is to obtain information about the mechanical bond strength along the interface between the borehole plug and borehole wall rock. The experimental procedure is illustrated in Fig. 1. A steel rod loads the plug axially until the plug is pushed down the borehole. During the standard push-out experiment, two variables are recorded: the displacement of the top of the plug and the load on the plug. The load and displacement values are plotted vs. each other to form the typical load-displacement curves (Fig. 2)

Over 100 of these tests were performed for two rock types, a Columbia Plateau basalt (Pomona flow) and Charcoal granite, used as host rock, and three expansive cements to form the plugs. Plug dimensions (length and diameter) were also varied. Material properties of the rocks and cements were determined, and a summary of these values is given in Table I. Frictional properties (cohesion and friction angle) of the rock-plug interface were determined by casting cement on rock at an angle which allows slip, and performing triaxial tests on the sample. The results indicate a friction angle and cohesion of approximately 40^{o} and 5 MPa, respectively, for all cement-rock interfaces.

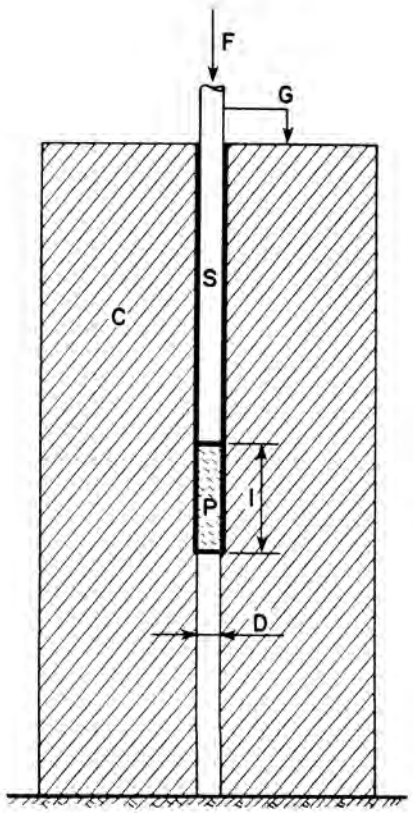

Fig. 1. Schematic illustration of push-out experiments. A steel rod (S) is used to apply a force (F) to one end of the plug (P) of diameter (D) and length (l) emplaced in a coaxial hole drilled in rock core (C). Displacement is measured by gage (G).

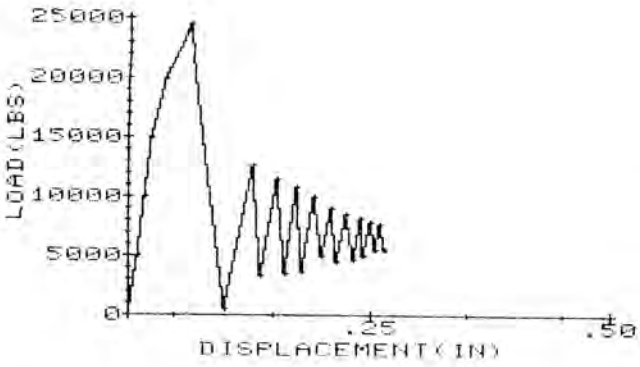

Fig. 2. Typical force-displacement curve generated by push-out test.

For some push-out tests, strain gages were mounted along the interior of the borehole wall to determine the axial strain induced in the rock as the cement plug was loaded. From the equilibrium of a plug section (Fig. 3):

$$\frac{d\sigma_x}{dx}\frac{d}{4} = \tau_x \ . \qquad (1)$$

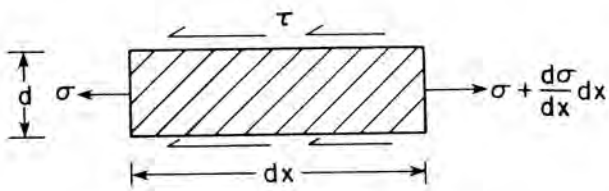

Fig. 3. Equilibrium of section of plug.

Provided the deformation is elastic, $\sigma_x = E\varepsilon_x$ so that Eq. (1) becomes:

$$\frac{d\varepsilon_x}{dx} E \frac{d}{4} = \tau_x \ . \qquad (2)$$

Hence, the shear stress distribution along the interface can be determined if sufficient strain measurements are made.

CLOSED-FORM SOLUTIONS

Shear Stress Distribution

The shear stress distribution for an axially loaded borehole plug (or any other cylindrical inclusion problem with similar boundary conditions) can be derived by assuming elastic behavior of both the plug and the rock.

As a compressive force is applied to the plug, load transfer through shear stresses will occur at the plug-rock interface. Because the deformations are assumed to be elastic $\varepsilon_x = dU/dx$, and Eq. (2) becomes:

$$\frac{d^2U_x}{dx^2} = \frac{4\tau_x}{dE} \qquad (3)$$

If the rock is thick ($R - a > a$), then τ_x is given by Farmer[3] as:

$$\tau_x = \frac{U_x\ G}{a \ln R/a} \ . \qquad (4)$$

Let

$$\alpha^2 = \frac{2G}{E\ a^2\ \ln R/a} \ . \qquad (5)$$

Substituting Eqs. (4) and (5) into (3) and solving the resulting differential equation yields:

$$U_x = \frac{\sigma_0}{E\alpha} \frac{\cosh \alpha (L - x)}{\sinh \alpha L} \ . \qquad (6)$$

The shear stress at any point along the plug-rock interface is determined by combining Eqs. (4) and (6):

$$\tau_x = \frac{\sigma_0 \alpha a}{2} \frac{\cosh \alpha (L - x)}{\sinh \alpha L} \ . \qquad (7)$$

Equation (7) indicates the shear stress distribution along the interface will be exponential. This is in agreement with theoretical and experimental results reported for mechanistically similar problems, e.g., rock bolts,[3] concrete reinforcement,[4] composite materials,[5] and rock socketed piers.[6]

Table I. Summary of Material Properties

Material	Young's Modulus (MPa)	Poisson's Ratio	Compressive Strength (MPa)
Hanford Basalt	6.7×10^4	.18	214 ± 42
Charcoal Granite	5.6×10^4	.19	123 ± 44
Cement System 1	7.6×10^3	.14	21 ± 3.5
Cement System 2	4.1×10^3	.23	4 ± 5
Cement System 3	6.9×10^3	.23	14 ± 7

Interface Strength

The plug-rock interface can be considered a discontinuity, and the relative motion between the cement plug and the wall rock will be shearing past one another. The maximum shear strength along the discontinuity is given by:[7]

$$\tau_x = c + \sigma_n \tan\phi \tag{8}$$

The cohesion and the friction angle were estimated from the cement-rock triaxial tests. The normal stress across the interface could have four components: change in lateral stressfield, dilatancy effects, expansive stresses generated by the cement, and the Poisson effect during loading. During the push-out experiments, no confining stresses were present and, because the borehole wall rock was smooth (all asperities less than 1 mm high), there was no normal stress produced by the tendency of the cement to dilate as it moves over the borehole wall rock.

The expansive stresses were measured for each cement type by curing the cement in steel pipes and measuring the induced tangential strain on the outside of the pipe with strain gages.[8] The stresses at eight days cure time, the cure time used for the push-out tests, ranged from .35 MPa to 2 MPa.

The Poisson effect is the tendency of the cement to expand laterally when an axial load is applied, thereby creating a normal stress across the interface. This normal stress can be determined by equating the plug and rock lateral displacements along the interface, and solving for the normal stress.

The lateral displacement in a plug being loaded axially is found from Hooke's Law, and the lateral displacement of the rock is calculated by use of hollow cylinder formulas.[7] Solving for the normal stress across the interface due to the Poisson effect yields:

$$\sigma_{np} = (NLF)\sigma_x \tag{9}$$

where

$$NLF = \frac{\nu_p E_R (R^2 - a^2)}{(1-\nu_p)E_R(R^2-a^2) + (1+\nu_R)E_p(a^2(1-2\nu_R) + R^2)} \tag{10}$$

The axial stress in the plug, σ_x, varies depending on the shear stress distribution along the interface. If the shear stress distribution is exponential and given by Eq. (7), then the axial stress in the plug is

$$\sigma_x = \sigma_o \frac{\sinh\alpha(L - x)}{\sinh\alpha L} \tag{11}$$

and the normal stress across the interface from the Poisson effect is

$$\sigma_{np} = NLF\,\sigma_o \frac{\sinh\alpha(L - x)}{\sinh\alpha L} \tag{12}$$

If the shear stress distribution is constant, the axial stress in the plug is given by

$$\sigma_x = (\sigma_o - \frac{\sigma_o}{L} x) \tag{13}$$

and the normal stress across the interface due to the Poisson effect is

$$\sigma_{np} = NLF\,\sigma_o (1 - \frac{x}{L}) . \tag{14}$$

The total strength of the interface can be determined by summing the strength at every point over the entire interface. This is accomplished by integrating over the surface of the plug, i.e.:

$$S = \int_0^L \int_0^{2\pi} \tau_x a\, d\theta dx . \tag{15}$$

Substituting Eq. (8) into Eq. (15) gives

$$S = \int_0^L \int_0^{2\pi} (c + \sigma_n \tan\phi)\, a\, d\theta dx . \tag{16}$$

If the shear stress distribution is exponential, then solving Eq. (16) yields

$$S = (c + \sigma_e \tan\phi)2\pi a L + \frac{2\pi a (NLF)\tan\phi\,\sigma_o (\cosh\alpha L - 1)}{\alpha \sinh\alpha L} . \tag{17}$$

If the shear stress distribution is constant, then Eq. (17) gives

$$S = (c + \sigma_e \tan\phi)2\pi a L + 2\pi a L (NLF)\frac{\sigma_o}{2} . \tag{18}$$

Both Eqs. (17) and (18) take the form

$$S = k_1 + k_2 F_o . \tag{19}$$

The strength, therefore, is a function of the applied load. When the strength equals the applied load, failure is defined. Equating S and F_o gives

$$S = \frac{k_1}{1 - k_2} \tag{20}$$

Solving Eq. (20) for appropriate values of k_1 and k_2 gives the maximum strength developed along the interface of a cylindrical inclusion using a frictional model to describe the interface strength.

Table II shows the predicted strengths from these calculations and the results from push-out experiments. The strengths calculated assuming an exponential shear stress distribution are usually closer to the experimental results than the strengths calculated assuming a constant shear stress distribution. Furthermore, assuming a constant shear stress distribution does not allow Eq. (20) to be solved with a positive number in some cases, implying mathematically infinite strength, which is clearly not plausible. Thus, for plugs prepared and tested under laboratory conditions, a frictional model of the interface strength, assuming an exponential shear stress distribution is reasonable.

Table II. Push-Out Results vs. Theoretical Results Using Frictional Model for Interface Strength for Cement System 2

Sample*	Theoretical Strength (N) for constant shear stress distribution	Theoretical Strength (N) for exponential shear stress distribution	Experimental Results (N)
Hanford Basalt 1.3-2.5	19,700	12,496	8900, 21,360
Hanford Basalt 1.3-5.1	379,545	25,253	26,700, 35,600
Hanford Basalt 1.3-10.2	-46,658	50,067	44,500, 55,625
Hanford Basalt 2.5-2.5	27,092	23,718	20,915
Hanford Basalt 2.5-5.1	77,982	47,824	35,600
Hanford Basalt 2.5-10.2	1,234,110	95,675	137,950, 109,025
Hanford Basalt 5.1-2.5	46,511	44,464	-
Hanford Basalt 5.1-5.1	105,634	89,610	93,450
Hanford Basalt 5.1-10.2	289,837	179,303	44,500, 35,600**
Charcoal Granite 1.3-2.5	19,393	13,683	6675, 35,155
Charcoal Granite 1.3-2.5	290,919	25,432	26,700, 13,350
Charcoal Granite 1.3-2.5	-48,474	50,863	68,975**, 57,850
Charcoal Granite 2.5-5.1	26,931	23,896	-
Charcoal Granite 2.5-5.1	76,531	48,358	26,700, 62,300, 33,375
Charcoal Granite 2.5-5.1	967,661	96,761	124,600, 93,450
Charcoal Granite 5.1-10.2	46,325	44,549	-
Charcoal Granite 5.1-10.2	104,677	89,997	48,950
Charcoal Granite 5.1-10.2	282,730	180,140	95,230**

*Numbers designate approximate diameter and length of plug in centimeters, respectively.

**Tensile failure of rock sample.

A more extensive discussion of the derivation of the equations in this section, assumptions involved, and resulting implications is given in Stormont[9] and Stormont and Daemen.[10]

IN-SITU PLUG BEHAVIOR

The frictional model assumes failure occurs instantaneously along the entire length of the plug, which is unlikely. In addition, the strength predicted by the frictional model increases rapidly with length, attaining very high values quickly. For longer plugs, it is more reasonable to assume failure is initiated when the maximum shear strength is exceeded locally.

The maximum shear stress for a given test could be determined if the axial strain distribution in either the rock or cement was known, as illustrated in Eq. (2). In addition, it is probable that the mode of failure - instantaneously along the length of the plug or locally initiated progressing along the length of the plug - could be identified. However, strain measurements have been troublesome to date (December 1982), and more work is required in this area.

Estimation of the maximum local shear strength is possible from a number of indirect ways. If the shear stress is given by Eq. (7), then the maximum occurs at $x = 0$ and is equal to:

$$\tau_{max} = \tau_{av} \alpha L \frac{\cosh \alpha L}{\sinh \alpha L} , \qquad (21)$$

where $\tau_{av} = F_o/2\pi rL$. As $\alpha \to 0$ in Eq. (21), $\tau_{max} \to \tau_{av}$.[5] Therefore, if τ_{av} is plotted vs. L (α held constant), an estimate of the shear strength can be obtained by extrapolating this plot to $L = 0$. This analysis proved inconclusive because of the wide scatter of the data, making extrapolation to $L = 0$ very difficult.

For the values of αL used in the push-out tests, $\cosh \alpha L / \sinh \alpha L \to 1$, rendering Eq. (21):

$$\tau_{max} = \alpha L \tau_{av} . \qquad (22)$$

Tabulation of the right hand side of Eq. (22) for the push-out tests shows great variability, from 7 MPa to 215 MPa. However, most values are in the range of 10 to 30 MPa.

An estimate of τ_{max} can be made by calculating the shear stresses on the cement-rock interface during triaxial tests on the composite samples. The shear stresses on the interface depend on the confining pressure. In the absence of confining pressure, the maximum shear stresses were on the order of 7 MPa.

When the confining pressure was increased to 20 MPa, the maximum shear stresses on the interface increased to 38 MPa. It appears likely that the maximum local shear strength along the plug-rock interface is in the range of 10 to 30 MPa, depending on the normal stress across the interface.

It is unlikely that the shear stresses will distribute over the entire length of a long plug. Rather, before failure there should be a length of plug beyond which no axial load should be present in the plug and therefore no shear stresses along the interface. Equation (12) predicts that the axial stress in a plug decreases to .1 % of the applied stress 7.5 cm. from the applied load for a 30.5 cm. long, 5.0 cm. diameter cement plug in Charcoal granite. Observations by Hawkes and Evans[4] during pull-out tests on rebar in concrete also confirm the finite distribution of shear stresses: "...practically all of the applied load has been transferred in the first 10 inches of embedded length (for a 18.5-inch long bar)." In addition, elastic solutions for soil stresses under a footing, such as those by Boussinesq and Westergard,[11] illustrate quite clearly that at a fairly shallow depth the influence from the surface load is negligible.

If the failure criterion is a maximum shear stress, failure should initiate at the top (loaded end) of the borehole plug. As slip occurs, the maximum shear stress moves down the interface in front of the failed (slip) zone. If there is residual strength along the failed portion of the interface, some load in the plug will be transferred to the rock in this zone. In this case, the maximum shear stress might decrease as it propagates along the interface. If the interface has no residual strength, then the maximum shear stress will not decrease as it propagates along the interface.

Therefore, a plug which has some residual strength along the plug-rock interface and which is longer than the length required for the pre-failure elastic shear stress distribution will experience an increase in strength upon initial failure. The continued decay of the maximum shear stress, through dissipation by residual stresses along the failed portion of the plug, will eventually lower the maximum shear stress below the shear strength if the plug is long enough.

This decrease in the maximum shear stress has been observed in a simple finite element model. The model consisted of plug, interface, and rock elements. The interface elements could experience progressive failure by the variable stiffness technique. The shear stresses are the difference between axial loads in the plug divided by the appropriate surface area. A maximum shear strength and residual shear strength (17.2 MPa and 5.2 MPa, respectively) were introduced as typical values associated with the push-out tests. Figure 4 shows the reduction in the maximum shear stress from 39 MPa in the first iteration to below 17 MPa in the fifth iteration.

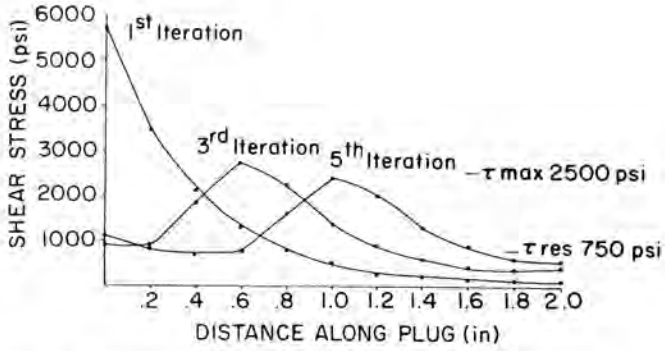

Fig. 4. Shear stress distributions generated by a finite element program which allowed progressive failure along the interface. Residual strength is 30% of peak strength.

CONCLUSIONS

Push-out experiments, performed on cement plugs of varying lengths and diameters, developed peak axial stresses in the range of 3.5 to 95 MPa. A statistical analysis produced no firm conclusions other than the strength usually increased with the length of the plug. In addition, these tests exhibited significant residual strength, usually in the range of 30-50% of the peak strength. The cements with a lower water content and greater expansive stresses generally develop higher residual strengths.

The shear stresses along the rock-plug interface are expected to be exponential. Strain distribution experiments, although not conclusive, indicate that the load is transferred rapidly over the initial portion of the plug. Elastic equations developed predict an exponential shear stress distribution, as do many other solutions proposed for mechanistically similar problems.

A frictional model for the interface strength, $\tau = c + \sigma\tan\phi$, predicts the strength reasonably well for laboratory testing. The assumption is made that the shear stresses are distributed exponentially along the plug-rock interface. Although the frictional model is probably not truly representative of the interface behavior, it allows identification of major components of interface strength: roughness of borehole wall, length of plug, material properties of rock and cement, and expansive stresses of the cement.

Borehole plugs emplaced at repository depths may have a greater strength than laboratory plugs if it is possible to duplicate the quality of the cement in a deep hole, which is unlikely due to segregation, mud contamination, etc. The increased strength is probable because in-situ plugs will be longer, the borehole wall may be rougher, and greater confinement is provided by the semi-infinite rock mass. If the existing stressfield changes, the stress across the interface will change, and hence the strength of the interface will change. This effect can either increase or decrease the strength, depending on the specific changes in the stressfield. For a discussion of this topic, see Jeffrey and Daemen.[12]

An in-situ plug will probably fail when a maximum local shear strength is exceeded. If residual strength is present along the failed portion of the plug and the plug is of sufficient length, the maximum shear stress will decrease as it propagates along the interface in front of the slip zone. This allows a borehole plug to increase in strength upon initiation of local failure.

It is unlikely that cement plugs installed in boreholes will be dislodged or will fail at pressure conditions likely to be encountered at planned repository depths. However, it was not possible to extrapo-

late any formulation or conclusions to tunnel and shaft sealing, a subject which has been identified as of significant importance in an isolation scheme.[13]

ACKNOWLEDGEMENT

This work is part of an ongoing research program, "Rock Mass Sealing," sponsored by the Waste Management Research Program Office of Nuclear Regulatory Research, U.S. Nuclear Regulatory Commission.

LIST OF SYMBOLS

- x - axial coordinate
- L - length of plug
- a - radius of plug
- d - diameter of plug
- R - radius of rock sample
- E_p - Young's modulus of plug material
- E_R - Young's modulus of rock
- ν_p - Poisson's ratio of plug material
- ν_R - Poisson's ratio of rock
- G - shear modulus of rock
- U_x - axial deformation of plug
- ε_x - axial strain in plug
- σ_x - axial stress in plug
- σ_n - normal stress across interface
- σ_{np} - normal stress across interface due to Poisson effect
- σ_e - normal stress across interface due to expansive stress
- F_o - applied axial force to plug
- σ_o - applied axial stress to plug
- τ_x - shear stress along interface
- τ_{max} - maximum shear stress along interface
- c - cohesion between cement and rock interface
- ϕ - friction angle between cement and rock interface
- S - theoretical strength of interface from frictional model
- k_1 - constant for given material and geometric properties
- k_2 - constant for given material and geometric properties.

REFERENCES

1. Klingsberg, C. and J. Duguid, 1980, "Status of Technology for Isolating High-Level Radioactive Wastes in Geological Repositories," DOE Office of Waste Isolation and Battelle Office of Nuclear Waste Isolation, DOE/TIC 11207 (draft), October.

2. ONWI-55, 1979, "Repository Sealing Design Approach 1979," D'Appolonia Consulting Engineers, Pittsburgh, PA 15235.

3. Farmer, I.V., 1975, "Stress Distribution Along a Resin Grouted Rock Anchor," Rock Mechanics Mining Science and Geomechanics Abstract, Vol. 12, pp. 347-351, Pergamon Press.

4. Hawkes, J.M. and R.H. Evans, 1951, "Bond Stresses in Reinforced Concrete Columns and Beams," Structural Engineer, Vol. 29, pp. 323-327, December.

5. Greszczuk, L.B., 1969, "Theoretical Studies of the Mechanics of the Fiber-Matrix Interface in Composites," Interfaces in Composites, ASTM STP 42, American Society for Testing and Materials, pp. 42-58.

6. Kulhawy, F.H. and R.E. Goodman, 1980, "Design of Foundations on Discontinuous Rock," Int. Conf. on Struct. Foundations, Sydney, May 7-9, Pells, ed., pp. 209-220.

7. Jaeger, J.C. and N.G.W. Cook, 1979, Fundamentals of Rock Mechanics, Chapman and Hall, London, John Wiley and Sons, Inc., New York, Third Edition.

8. South, D.L., W.B. Greer, N.I. Colburn, S.L. Cobb, B. Kousari, S.P. Mathis, R.G. Jeffrey, C.A. Wakely, and J.J.K. Daemen, 1982, "Annual Report, Rock Mass Sealing, June 1, 1981 - May 31, 1982," Prepared for U.S. Nuclear Regulatory Commission, SAFER Division by Nuclear Fuel Cycle Research Program, Dept. of Mining and Geological Engineering, University of Arizona, Tucson, AZ.

9. Stormont, J., 1983, "Mechanical Strength of Borehole Plugs," M.S. Thesis, Dept. of Mining and Geological Engineering, University of Arizona, Tucson, AZ.

10. Stormont, J. and J.J.K. Daemen, 1983, "Mechanical Strength of Borehole Plugs," Topical Report to U.S. Nuclear Regulatory Commission, SAFER Division, Office of Nuclear Regulatory Research.

11. Sowers, G.F., 1979, Introductory Soil Mechanics and Foundations, Macmillan Publishing Co., New York.

12. Jeffrey, R.G. and J.J.K. Daemen, 1981, "Shaft or Borehole Plug-Rock Mechanical Interaction," in Proceedings of the Symposium on Waste Management, Tucson, Arizona, February.

13. Kelsall, P.C. and D.K. Shukla, 1980, "Shaft and Tunnel Sealing Considerations," OECD Nuclear Energy Angency and United States Department of Energy Workshop on Borehole and Shaft Plugging, Columbus, Ohio, May.